AJNR

Combined Fat- and Water-Suppressed MR Imaging of Orbital Tumors

Alan Jackson, Scott Sheppard, Andrew C. Johnson, Deborah Annesley, Roger D. Laitt and Andrea Kassner

AJNR Am J Neuroradiol 1999, 20 (10) 1963-1969
http://www.ajnr.org/content/20/10/1963

AJNR Am J Neuroradiol 20:1963–1969, November/December 1999

Combined Fat- and Water-Suppressed MR Imaging of Orbital Tumors

Alan Jackson, Scott Sheppard, Andrew C. Johnson, Deborah Annesley, Roger D. Laitt, and Andrea Kassner

BACKGROUND AND PURPOSE: **The use of a high-resolution T2-weighted MR sequence, which suppresses signal from both fat and water, has been shown to be highly effective for depicting areas of inflammatory damage within the optic nerve. The ability of this sequence to show neoplastic and inflammatory orbital lesions, which may mimic neuritis, is unknown. This study was designed to examine the characteristics of such a sequence for the investigation of orbital mass lesions.**

METHODS: **Twenty-eight patients with known or suspected mass lesions of the orbit and six healthy volunteers were recruited for study. Imaging was performed with a 1.5-T MR unit. Participants were examined by selective partial inversion recovery (SPIR) sequences with T2-weighted fast spin-echo acquisition, selective partial inversion recovery/fluid attenuated inversion recovery (SPIR/FLAIR) sequences with fast spin-echo acquisition, short tau inversion recovery (STIR) sequences with fast spin-echo acquisition, and SPIR sequences with contrast-enhanced T1-weighted fast spin-echo acquisition. Two neuroradiologists, using a randomised, blinded method, scored images for lesion presence and extent. Lesion extent was defined as the number of images with visible abnormality, and was compared with the standard of reference established at a later date by consensus review of all imaging sequences. The ability of the sequences to show the presence and extent of pathologic lesions was compared.**

RESULTS: **The SPIR/FLAIR sequence showed both the presence and extent of orbital masses significantly better than did either STIR or T2-weighted SPIR sequences ($P<.01$ and $P<.001$, respectively). Contrast-enhanced T1-weighted SPIR images ranked better than SPIR/FLAIR images, although the difference failed to reach statistical significance. In the orbital apex, the SPIR/FLAIR technique was superior to all other techniques used. This reflected its ability to distinguish enhancing, pathologic lesions from enhancing, normal anatomy.**

CONCLUSION: **SPIR/FLAIR is an appropriate screening technique for orbital masses and offers significant advantages over currently used fat-suppressed sequences for the investigation of orbital disease.**

High-resolution MR imaging of the orbit has become an accepted diagnostic technique for a wide range of orbital disease (1–3). MR imaging of the orbit, however, often is not performed for a number of reasons. First, CT provides an excellent alternative technique for imaging the orbit. The speed of CT allows motion-free imaging and routine use of high spatial resolution enables the identification of small anatomic and pathologic features. In addition, the presence of large amounts of fat within the orbit produces high contrast, allowing the use of low-radiation dose protocols (4–6). In contrast, many difficulties are encountered with the use of high-resolution MR for the imaging of the orbit (7). In particular, extensive fat in the orbit is problematic. The resonant frequency of protons bound to fat differs from that of protons bound to water by 220 Hz (at 1.5 T). This variation in resonant frequency causes spatial misregistration of the fat image in the phase-encoding direction (chemical shift artifact) (7, 8). The result of chemical shift artifact is variations in signal intensity at fat-water boundaries. Equally important is the high signal intensity arising from fat that decreases the dynamic range of the non-fat areas of the images (9) and obscures enhancing lesions after contrast medium administration (10).

Received in original form October 8, 1998; accepted after revision March 22, 1999.

From the Department of Diagnostic Radiology (A.J., A.C.J., D.A.) University of Manchester, Manchester, UK; Philips Medical Systems (A.K.), Hammersmith, UK; Emory University, Atlanta, GA and Philips Medical Systems (S.S.), Shelton, CT; and the Department of Neuroradiology, Manchester Royal Infirmary, Manchester, UK.

Address reprint requests to Professor A Jackson, Dept of Diagnostic Radiology, University of Manchester, Oxford Rd, Manchester, M13 9PT, UK.

These problems have led to the routine use of fat-suppression techniques in orbital imaging for both enhanced and unenhanced images (9–17). The use of fat-suppression methods is of particular benefit in contrast-enhanced T1-weighted imaging and has become the standard method for postcontrast imaging in many institutions (10, 18). The benefit of fat suppression is the increase of contrast between enhancing lesions and the surrounding normal tissue, which is usually predominantly fat.

In unenhanced images, the development of fat-suppression techniques has been studied most extensively for the investigation of optic neuritis (13, 14, 16, 19). The identification of high-signal lesions within the optic nerve on T2-weighted images is improved by suppression of the fat signal in the surrounding orbit (16). Both short tau inversion recovery (STIR) and selective partial inversion recovery (SPIR) techniques appear to be effective to varying degrees.

STIR sequences suppress fat signal by using an initial 180° radiofrequency pulse to invert the longitudinal magnetization. Image acquisitions then are performed with the inversion time equivalent to the null point for fat (approximately 0.69 × T1) (20). The major disadvantages of the STIR sequence are the high signal produced by CSF and the tendency of the sequence to suppress signal from other substances with short T1 relaxation times. These limitations led to the development of fat-suppression techniques based on the use of frequency-specific SPIR pulse sequences (21, 22). In these sequences, a frequency-specific inversion pulse inverts only the fat magnetization while leaving water resonances undisturbed (19). This technique can be used with a wide range of pulse sequences and will not suppress areas of T1 shortening caused by contrast enhancement, allowing its use in combination with postcontrast T1-weighted acquisitions. SPIR sequences reliably differentiate fat from tissues with T1 values similar to that of fat and do not alter the contrast between normal non-fatty tissues. The SPIR technique is extremely sensitive to magnetic field inhomogeneity. The use of an automatic shimming algorithm prior to each acquisition minimizes magnetic field inhomogeneity and facilitates satisfactory fat suppression across large image volumes.

Both STIR and T2-weighted SPIR images suffer from the presence of high signal from CSF in the optic nerve sheath. We recently described a heavily T2-weighted sequence, which combined SPIR fat suppression with a fluid attenuated inversion recovery (FLAIR) sequence to produce combined fat and water suppression. This SPIR/FLAIR sequence has proved clearly superior to either STIR or T2-weighted SPIR imaging for the visualization of optic neuritis (19).

The choice of imaging sequences for the investigation of suspected optic neuritis relies on the ability of the sequence to depict both neuritic segments and other orbital disease that may mimic a neuritic process. The aim of this study was to assess whether the SPIR/FLAIR sequence can enable reliable identification of mass lesions within the orbit.

Methods

Using the SPIR/FLAIR sequence, imaging was performed in six healthy volunteers (three men, three women; aged 23–42 years [median age, 27 years]) to demonstrate the appearance of the normal orbit. These examinations were used only for reference during reporting and were not included in the study. In addition, imaging was performed in 28 patients with a known (n=12) or suspected (n=16) orbital mass. Two of the 28 patients studied were imaged on two occasions so that 30 clinical scan series were entered into the investigation. Nineteen patients were women and nine were men, aged 18–73 years (median age, 46 years).

Imaging was performed on a 1.5-T scanner. T1-weighted localizer images were performed in the axial, sagittal, and coronal planes. High-resolution T1-weighted axial-volume acquisition with 1.5-mm partitions (29/20 [TR/TE]; field of view, 200 mm^2; matrix, 256^2) was performed in all cases to allow the selection of the optimal imaging plane (7). Subsequent imaging performed in patients was acquired in either the coronal or axial planes based on the appearance of the lesion on the initial T1-weighted image. Subsequent imaging was performed in healthy volunteers in the axial plane in three and in the coronal plane in three. All study participants were imaged using 3D fast spin-echo (FSE) fat-suppressed sequences incorporating a SPIR preparation pulse. These were: 1) T2-weighted SPIR (3085/120 [TR/TE]; field of view, 180mm^2; matrix, 512^2; signal average, 5; echo train length, 12; imaging time, 4 minutes 25 seconds); 2) T2-weighted with combined fat and water suppression SPIR/FLAIR (8000/120 [TR/TE]; TI, 2200; field of view, 160mm^2; matrix, 256^2; signal average, 2; echo train length, 21; imaging time, 4 minutes); and 3) postcontrast T1-weighted postcontrast SPIR (450/20 [TR/TE]; field of view, 160 mm^2; matrix, 256^2; signal average, 2; echo train length, 4; imaging time, 3 minutes 16 seconds). An FSE STIR sequence also was performed(1560/50 [TR/TE]; TI, 165; field of view, 180 mm^2; matrix, 256^2; signal average, 2; echo train length, 4; imaging time, 2 minutes 41 seconds). All four fat-suppressed sequences used 3-mm slices with 0.3-mm interslice gaps. The STIR and SPIR sequences were based on the technique described by Gass et al (16) with reduction of the field of view to give an in-plane resolution of 0.7 mm for STIR and 0.35 mm for SPIR. The decreased resolution of the STIR sequences reflects the increase in imaging time required for the inversion pulse. These limitations are greater with the SPIR/FLAIR sequences owing to the longer inversion and repetition times. In this study, these drawbacks were offset by an increase in the echo train length of the FSE collection.

Additional sequences were performed in 18 patients. These included MR angiography in one patient and additional images in alternative planes to aid in the surgical planning of 17 patients. In addition, all patients underwent axial T2-weighted imaging of the brain to exclude significant cerebral disease (gradient spin-echo [23]: 3622/90 [TR/TE]; 90°; echo-planar factor, 3; echo train length, 4; 2 repetitions).

Image Assessment

All fat-suppressed clinical images were assessed from hardcopy by two experienced neuroradiologists (RJD and AJ). The radiologists performed the reporting independently and in a blinded manner. Using one imaging sequence only, each undertook four reporting sessions during which they assessed images from all patients. The ability of the sequences to depict disease was assessed using a simple, subjective grading system (0, all images normal; 1, possible abnormality; 2, probable

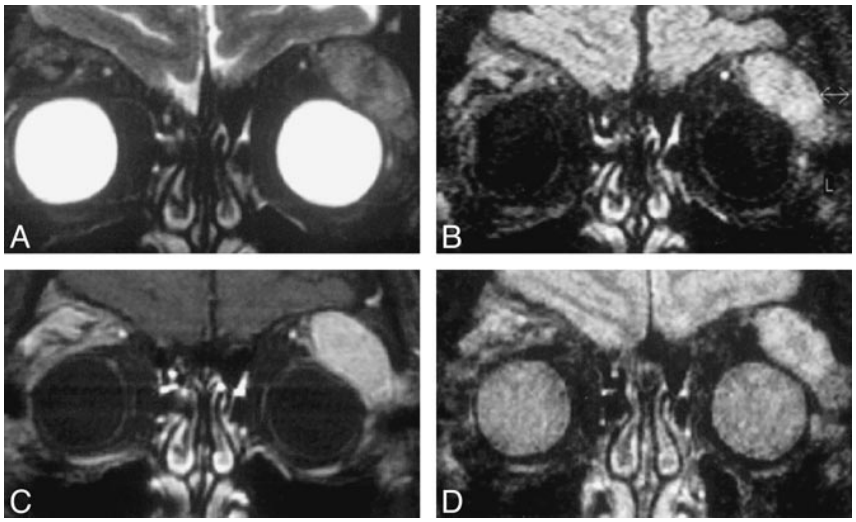

FIG 1. Coronal images through the orbits of a patient with lymphoma of the lacrimal gland. Sequences are T2-weighted SPIR (*A*), SPIR/FLAIR (*B*), T1-weighted SPIR with contrast (*C*), and STIR (*D*).

abnormality; 3, definite abnormality). Abnormality was defined as the presence of an abnormal mass lesion on any image. Images obtained from healthy volunteers were used for comparison.

In addition, the extent of the lesion as shown by each sequence also was assessed. This was performed on separate occasions after the initial scoring. The radiologists again performed the reporting independently and in a blinded manner over four separate, sequence-specific reporting sessions. The extent of the lesion was recorded as the number of images showing abnormality. In order to assess the ability of individual sequences to illustrate lesion extent, these scores were compared to the maximal extent of the lesion, as shown by combined examination of all available imaging sequences. This standard-of-reference measurement of extent was determined by consensus between two radiologists (RDL and AJ) at a final, separate reporting session. The accuracy with which the individual, fat-suppressed sequences displayed the standard-of-reference measurement of lesion extent then was scored as: 0, lesion not shown; 1, less than half of the lesion visible; 2, more than half the lesion shown; 3, full extent of the lesion shown.

Analysis of Results

Interobserver reliability of lesion scoring was assessed using a weighted Cohen's kappa test (24). For comparative statistical analysis, the scores for lesion visibility and extent for each patient were ranked as follows. The scores obtained for lesion visibility on individual sequences were ranked so that the highest scores, indicating the greatest confidence that a lesion was present, ranked 1 (best visibility) to 4 (worst visibility). A similar ranking was applied to scores of lesion extent so that the sequence, which showed the greatest extent compared with the standard of reference, ranked 1 (greatest extent) to 4 (least extent). A mean rank then was calculated for each sequence so that a mean rank score of 1 would indicate that a sequence performed better than all other sequences with which it was compared in all patients. Ranking values were used to calculate significance by a rank-order statistical method (24). In addition, a similar analysis was performed on each of three subgroups: 1) lesions in the globe or preseptal area (n = 10); 2) postseptal lesions that do not extend to the apex (n = 9); and 3) lesions involving the orbital apex (n = 11). These subdivisions were selected because the local anatomy in each of these areas might be expected to effect the efficiency of the combined fat- and water-suppression sequence in comparison with sequences using fat suppression alone.

The use of mean-ranking scores can be potentially misleading because outliers may exist if sequences perform in a non-representative way in small numbers of patients. In order to avoid these errors, the rank scores from individual cases were reviewed to identify any in which the mean rankings were not representative. All cases in which the rank orders of any of the sequences differed by more than 1 from the mean values calculated for the entire patient group are described individually in the following results.

Results

Interobserver reliability for subjective scores of abnormality was excellent (kappa = .83). In two of the 28 cases, the clinical diagnosis of an orbital tumor was not confirmed by imaging with unexpected diagnoses of optic and oculomotor neuritis. In the remaining 26 cases, the presence of an orbital mass lesion was confirmed. Radiologic diagnoses were histologically confirmed in 23 cases. These 23 cases consisted of idiopathic orbital inflammatory syndrome (n=6), orbital meningioma (n=4), ocular melanoma (n=2), orbital melanoma (n=1), lymphoma (n=3), schwannoma (n=3), breast metastasis (n=1), cavernous hemangioma (n=3), and dermoid cyst (n=1). In five cases, the presumed diagnoses were based on clinical and radiologic features. These included choroidal hemangioma (n=1), optic neuritis (n=1), oculomotor neuritis (n=1), optic nerve glioma (n=1), and oculomotor tumor (n=1).

The image quality of the SPIR/FLAIR images was good in all cases. Signal-to-noise ratios of SPIR/FLAIR sequences were poor compared with T2-weighted imaging with SPIR and T1-weighted postcontrast imaging with SPIR. The increased T2-weighting possible with the SPIR/FLAIR sequence, however, produced improved contrast between tumor and normal tissue in most cases (Fig 1). The SPIR/FLAIR images showed lesions in all cases. Fat suppression was homogeneous throughout the orbits in all cases. The comparative rankings of the four fat-suppressed sequences are shown in Table 1. The SPIR/FLAIR sequence (sequence 3; mean rank, 1.34) and T1-weighted SPIR sequence with contrast medium administration (sequence 4; mean

Mean rankings for presence and extent of abnormality for the whole orbit and by orbital region

Anatomic Area	Whole Orbit (n = 30)		Globe and Pre-Septal (n = 10)		Retrobulbar (n = 9)		Orbital Apex (n = 11)	
	Presence of Abnormality	Extent of Abnormality	Presence of Abnormality	Extent of Abnormality	Presence of Abnormality	Extent of Abnormality	Presence of Abnormality	Extent of Abnormality
Sequence								
T2 SPIR	2.14	2.34	2.2	2.4	2.42	2.35	2.02	2.11
SPIR/FLAIR	1.34	1.66	1.55	1.63	1.58	1.89	1.2	1.49
T1 SPIR with Contrast	1.32	1.58	1.50	1.56	1.58	1.79	1.88	1.73
STIR	1.93	2.04	2.1	2.0	2.13	2.2	1.76	2.14

Note.—The rank score indicates the relative performance of the sequence compared with other sequences. A rank of 1 would indicate that the sequence performed consistently better than the other three sequences.

rank, 1.32) were ranked significantly higher for lesion identification than were the T2-weighted SPIR (sequence 2; mean rank, 2.14) and STIR sequences (sequence 5; mean rank, 1.93; $P < .01$). Comparison of lesion extent, as revealed by the four sequences (Table 1), produced a similar result ($P < .01$).

Table 1 also shows the comparison of the sequence performance in different areas of the orbit. These results show a similar pattern to those for the orbit as a whole with lesions in the anterior (globe and preseptal area) and the retrobulbar orbit. In the orbital apex, the SPIR/FLAIR sequences performed significantly better in the identification of abnormality than did the other sequences (mean rank, 1.21; $P < .001$). The T1-weighted SPIR sequences with contrast medium administration (sequence 4; mean rank, 1.88) were ranked significantly lower in the orbital apex than in the other orbital areas because of difficulty in separating small-enhancing, apical lesions from normal-enhancing, apical structures.

Review of the rankings revealed three cases in which the SPIR/FLAIR sequence depicted significant presence of disease not seen on other sequences. In one case (oculomotor neuritis), the SPIR/FLAIR sequence was the only one to show a pathologic lesion. In the case of optic neuritis, abnormal nerve signal was identified on SPIR/FLAIR, STIR, and T2-weighted SPIR images but was far more extensive on SPIR/FLAIR sequences involving the nerve in areas apparently normal on other sequences. In a third case (Fig 2), the SPIR/FLAIR sequence was the only one to show optic neuritis distal to an orbital apex meningioma. The meningioma itself was visible on all sequences.

Review of individual cases identified only three in which the rank order differed from the mean rank order by 1 or more. The first of these was a small melanotic melanoma with an associated retinal detachment. In this case, the SPIR/FLAIR sequence did not clearly show the tumor itself, although tumor was seen on the T2-weighted and STIR images (Fig 3). In the second case, the intracranial en plaque spread of an orbital apex meningioma was not appreciated on the SPIR/FLAIR sequence. It was well seen on T1-weighted SPIR sequences with contrast medium administration because of tumor enhancement and on the T2-weighted SPIR and STIR sequences where it was outlined by high-signal CSF (Fig 4). In the third case, areas of central high signal in an optic nerve meningioma were visible by both T2-weighted SPIR and STIR imaging but were not seen on SPIR/FLAIR images (Fig 5). Histologic analysis revealed this area corresponded to an area of cystic necrosis with tumor debris.

Discussion

The original rationale for the development of the SPIR/FLAIR sequence was to improve the conspicuity of neuritic segments of the optic nerve by suppression of surrounding CSF and fat. Although the sequence proved clearly superior to other fat-suppression methods (19), its routine use in suspected optic neuritis can be recommended only if it also can adequately reveal other orbital lesions.

The findings of the present study indicate that the SPIR/FLAIR sequence provides a reliable method for the demonstration of orbital masses. More surprisingly, the SPIR/FLAIR sequence was found to be significantly better than either STIR or T2-weighted SPIR imaging at depicting both the presence and extent of lesions. This result was unexpected because there seems little reason why fluid suppression should improve the visualization of orbital masses that are neither cystic nor adjacent to CSF. Indeed, the requirement for a long TR in the SPIR/FLAIR sequence produces images with lower signal-to-noise ratios than do either STIR or T2-weighted SPIR images. Furthermore, restrictions on imaging time allow the T2-weighted SPIR sequence to be implemented routinely with a much higher spatial resolution than that achieved with either STIR or SPIR/FLAIR imaging. Two reasons for the superior performance of the SPIR/FLAIR sequence can be identified. First, the suppression of fluid signal allows the use of a higher degree of T2 weighting than is possible with conventional T2-weighted SPIR sequences, as is evident in Figures 1A and 1B. A lacrimal gland lymphoma is far brighter on the SPIR/FLAIR image than on the T2-weighted SPIR image in which fluid contributes the

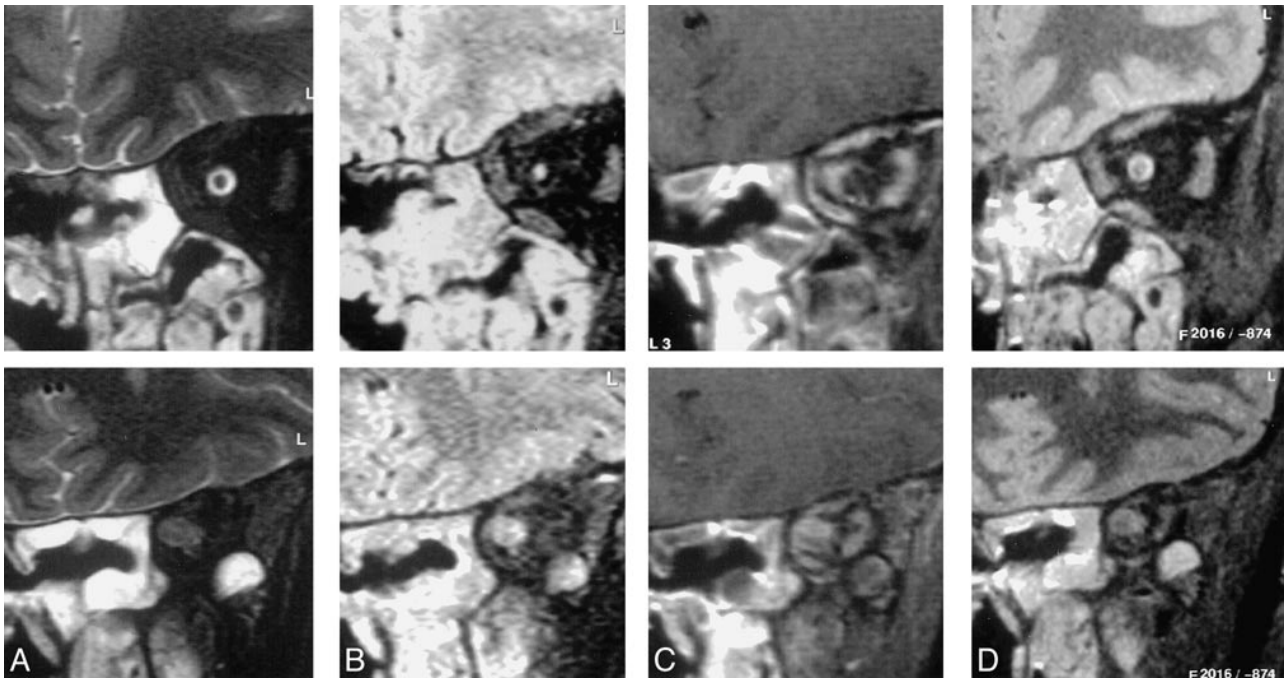

FIG 2. Coronal images through the orbits of a patient with an orbital apex meningioma. The sequences are T2-weighted SPIR (*A*), SPIR/FLAIR (*B*), T1-weighted SPIR with contrast (*C*), and STIR (*D*).

Images in the mid orbit (*top row*) show normal appearances on the STIR (top of *D*) and T2-weighted SPIR (*top of A*) images. The SPIR/FLAIR image (*top of B*) clearly shows increased signal in the optic nerve itself. Postcontrast T1-weighted SPIR (*top of C*) shows thickening of the optic nerve sheath because of meningioma en plaque. Images at the orbital apex (*bottom row*) demonstrate a mass lesion in the position of the optic nerve–sheath complex. The contrast between the lesion and surrounding tissues is greater on the SPIR/FLAIR image (*bottom of B*) than on the T2-weighted SPIR (*bottom of A*) or STIR (*bottom of D*) images. On the postcontrast T1-weighted SPIR image (*bottom of C*) the lesion shows inhomogeneous enhancement and is difficult to distinguish from adjacent enhancing extraocular muscles.

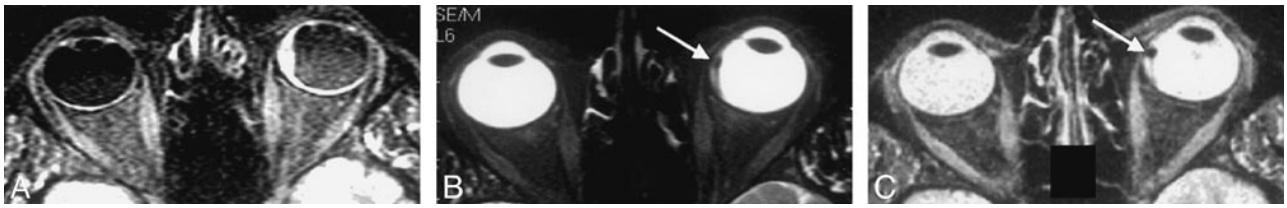

FIG 3. Axial images through the globe in a patient with a small melanotic melanoma with an associated retinal detachment. The SPIR/FLAIR sequence (*A*) shows the extent of the detachment more clearly than the T2-weighted SPIR (*B*) and STIR images (*C*), but does not reveal the tumor itself.

brightest signal. Although this is, in part, a true reflection of the increase in T2 weighting, the absence of fluid signal on FLAIR/SPIR images also increases the dynamic range for remaining tissues in the image and allows the routine use of narrower display windows. A similar effect was described by Flanders et al (9) who reported improved conspicuity of lesions within the globe when fat suppression was employed, even though no fat was present in or adjacent to the lesions themselves.

In three cases, SPIR/FLAIR images depicted pathologic lesions that were not seen on other images. In each of these, the lesion was a neuritic segment of either the optic or oculomotor nerves. In one case (Fig 2) this neuritic process was secondary to a small, apical meningioma proximal to signal abnormality in the optic nerve. In another, it was owing to cerebral lupus erythematosis, and more widespread abnormalities were apparent on the brain images. The exquisite sensitivity of the SPIR/FLAIR sequence to neuritic processes must be appreciated if the sequence is to be used in clinical practice. Compressive or vascular neuropathies may be secondary to a wide range of disease processes and may not be the prime abnormality (18, 25). The detection of an area of high signal within a nerve on SPIR/FLAIR images should therefore lead to a careful review of the images for lesions that may lead to this as a secondary change.

SPIR/FLAIR sequences performed poorly in three cases. In the first of these, a small, pigmented melanoma within a hemorrhagic retinal detachment was hardly visible because of partial volume averaging (Fig 3). This reflects a disadvantage of the combination of increased T2-weighting and low spatial resolution. In the second case, the presence

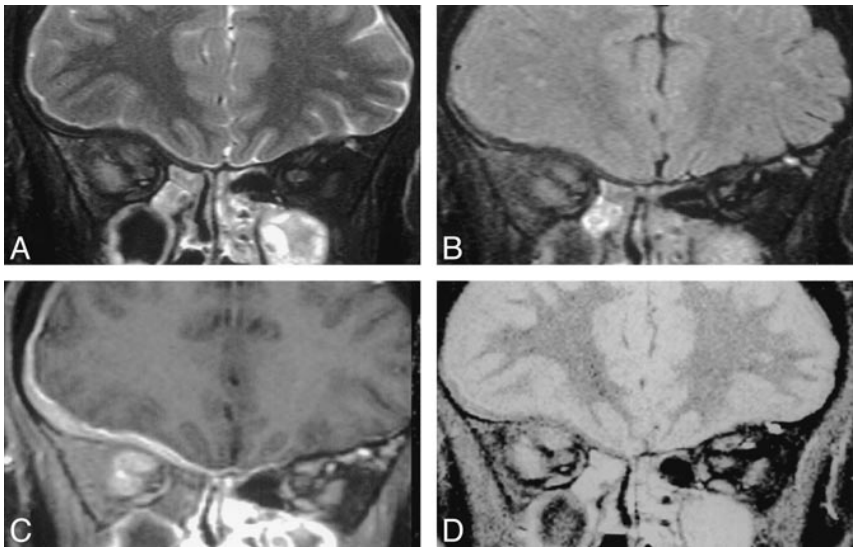

FIG 4. Coronal images through the orbit in a patient with an orbital apex meningioma. The extensive intracranial en plaque spread is shown well on the T1-weighted SPIR sequence with contrast (*C*) and also can be appreciated on the T2-weighted SPIR (*A*) and STIR (*D*) images it is outlined by high-signal CSF. Although the meningeal thickening can be seen on the SPIR/FLAIR sequences (*B*), its presence and extent were not appreciated by either of the radiologists who were reporting on this scan in isolation.

of intracranial en plaque spread of a meningioma was not appreciated on the SPIR/FLAIR sequences (Fig 4). This presumably reflects decreased conspicuity of the meningeal lesion that was outlined by high-signal CSF on other fat-suppressed sequences. Finally, an area of cystic necrosis within an orbital meningioma was not visible on the SPIR/FLAIR images, presumably reflecting reduced signal from fluid suppression (Fig 5).

In comparison with postcontrast T1-weighted SPIR images, the SPIR/FLAIR sequence again performed unexpectedly well. Although SPIR/FLAIR ranked lower than contrast-enhanced T1-weighted SPIR images, the difference did not reach statistical significance. The extent of disease shown by T1-weighted SPIR imaging was under-represented by SPIR/FLAIR sequences in only one case. This finding occurred with the same patient described above in whom SPIR/FLAIR under-represented the intracranial meningeal extent of an orbital apex meningioma (Fig 4). More surprisingly, the SPIR/FLAIR sequence outperformed the enhanced T1-weighted SPIR sequence in the orbital apex by improving the differentiation between normal structures and tumor.

We have suggested previously that the SPIR/FLAIR sequence should be used routinely in the investigation of suspected optic neuritis (19). On the basis of this study, we would also suggest the routine use of a T2-weighted SPIR/FLAIR sequence in the investigation of suspected orbital masses. The SPIR/FLAIR sequence can replace STIR or T2-weighted fat-suppressed images without loss of diagnostic specificity and will, in some cases, depict disease such as optic neuritis, which would not otherwise be seen. We believe that postcontrast T1-weighted images with fat suppression should also be routinely used because they provide increased sensitivity to masses in the middle and anterior orbit.

Conclusion

The demonstration of orbital masses with SPIR/FLAIR imaging is superior to that of other fat-suppressed, non-contrast, enhanced sequences. In the orbital apex, SPIR/FLAIR images provide delineation of normal and pathologic structures superior to both non-contrast and contrast-enhanced images. The SPIR/FLAIR sequence therefore offers significant advantages over currently used fat-suppressed sequences for the investigation of orbital disease.

Acknowledgment

We thank Philips Medical Systems for their support of this investigation.

References

1. Dorfman RE, Spickler EM. **Current status of magnetic resonance imaging of the orbit.** *Top Magn Reson Imaging* 1990;2: 17–26

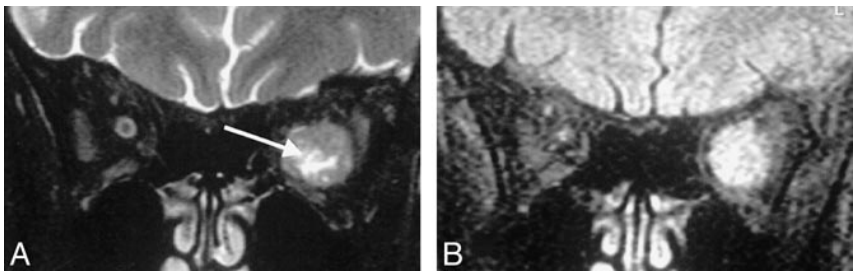

FIG 5. Coronal images in a patient with an orbital meningioma. A central area of cystic necrosis visible on T2-weighted SPIR images (*A, arrow*) is not apparent on SPIR/FLAIR images (*B*).

2. De Potter P, Flanders AE, Shields CL, Shields JA. **Magnetic resonance imaging of orbital tumors.** *Int Ophthalmol Clin* 1993; 33:163–173
3. Mafee MF, Inoue Y, Mafee RF. **Ocular and orbital imaging.** *Neuroimaging Clin N Am* 1996;6:291–318
4. Jackson A, Whitehouse RW. **Low-dose computed tomographic imaging in orbital trauma.** *Br J Radiol* 1993;66:655–661
5. Goodall KL, Jackson A, Leatherbarrow B, Whitehouse RW. **Enlargement of the tensor intermuscularis muscle in Graves' ophthalmopathy. A computed tomographic and magnetic resonance imaging study.** *Arch Ophthalmol* 1995;113:1286–1289
6. Whitehouse RW, Batterbury M, Jackson A, Noble JL. **Prediction of enophthalmos by computed tomography after 'blow out' orbital fracture.** *Br J Ophthalmol* 1994;78:618–620
7. Herrick RC, Hayman LA, Taber KH, Diaz-Marchan PJ, Kuo MD. **Artifacts and pitfalls in MR imaging of the orbit: a clinical review.** *Radiographics* 1997;;17:707–724
8. Whitehouse RW, Hutchinson CE, Laitt R, Jenkins JP, Jackson A. **The influence of chemical shift artifact on magnetic resonance imaging of the ligamentum flavum at 0.5 tesla.** *Spine* 1997;22: 200–202
9. Flanders A, DePotter P, Rao V, Vinitski S, Tom B, Sheilds J, Sheilds C. **Improved visibility of intraocular neoplasia using fat supressed, contrastenhanced MRI.** *Int J Neuroradiol* 1996; 2:339–346
10. Barakos JA, Dillon WP, Chew WM. **Orbit, skullbase, andpharynx: contrast-enhanced fat suppression MR imaging.** *Radiology* 1991;179:191–198
11. Atlas SW, Grossman RI, Hackney DB, Goldberg HI, Bilaniuk LT, Zimmerman RA. **STIR MR imaging of the orbit.** *AJR Am J Roentgenol* 1988;151:1025–1030
12. Tien RD, Chu PK, Hesselink JR, Szumowski J. **Intra- and paraorbital lesions: value of fat-suppression MR imaging with paramagnetic contrast enhancement.** *AJNR Am J Neuroradiol* 1991;12:245–253
13. Johnson G, Miller DH, MacManus D, Tofts PS, duBoulay E, McDonald WI. **STIR sequences in NMR imaging of the optic nerves.** *Neuroradiology* 1987;29:238–245
14. Guy J, Mao J, Bidgood WD Jr, Mancuso A, Quisling RG. **Enhancement and demyelination of the intraorbital optic nerve. Fat suppression magnetic resonance imaging.** *Ophthalmology* 1992;99:713–719
15. Tartaro A, Onofrj M, Thomas A, Fulgente T, Delli Pizzi C, Bonomo L. **Long time echo stir sequence magnetic resonance imaging of optic nerves in optic neuritis.** *Eur J Radiol* 1995;19: 155–163
16. Gass A, Moseley IF, Barker GJ, Jones S, MacManus D, McDonald WI, Miller DH. **Lesion discrimination in optic neuritis using high-resolution fat-suppressed fast spin-echo MRI.** *Neuroradiology* 1996;38:317–321
17. Hendrix LE, Kneeland JB, Haughton VM, Daniels DL, Szumowski J, Williams AL, Mark LP, Czervionke LF. **MR imaging of optic nerve lesions: value of gadopentetate dimeglumine and fat-suppression technique.** *AJNR Am J Neuroradiol* 1990;11: 749–754
18. Jackson A, Fawcitt R. **Orbital imaging.** In: Magnetic Resonance Imaging and Computed Tomography of the Head and Neck. Gillespie J, Gholkar A, eds. London: Chapman and Hall Medical; 1994;71–82
19. Jackson A, Sheppard S, Kassner A, Moriarty D. **Optic neuritis: MR imaging with combined fat and water suppression techniques.** *Radiology* 1998;206:57–63
20. Tartaro A, Onofrj M, Delli Pizzi C, Bonomo L, Thomas A, Fulgente T, Gambi D. **Long time echo STIR sequence magnetic resonance imaging of optic nerves in optic neuritis.** *Ital J Neurol Sci* 1996;17:35–42
21. Tien RD. **Fat-suppression MR imaging in neuroradiology: techniques and clinical application.** *AJR Am J Roentgenol* 1992; 158:369–379
22. Oh CH, Hilal SK, Cho ZH. **Selective partial inversion recovery (SPIR) in steady state for selective saturation magnetic resonance imaging (MRI)[abstract].** *Magn Reson* 1988;;–324
23. Oshio K, Feinberg DA. **GRASE (Gradient- and spin-echo) imaging: a novel fast MRI technique.** *Magn Reson Med* 1991;20: 344–349
24. Altman D. **Practical Statistics for Medical Research.** London: Chapman Hall; 1991;
25. Sklar EML, Schatz NJ, Glaser JS, Post JD, Hove MT. **MR of vasculitis induced optic neuropathy.** *AJNR Am J Neuroradiol* 1996;17:121–128